Exosome-Mediated Transfer of circRNA-GLIS3 Enhances Temozolomide Resistance in Glioma Cells Through miR-548m/MED31 Axis

Guowei Li
Second Affiliated Hospital of Soochow University https://orcid.org/0000-0001-9850-612X
YanPing Jin (gwli19880729@stu.suda.edu.cn)
Second Affiliated Hospital of Soochow University https://orcid.org/0000-0003-1905-2540

Primary research

Keywords: TMZ resistance, glioma, circRNAs, progression, apoptosis, axis, target.

Posted Date: May 11th, 2021

DOI: https://doi.org/10.21203/rs.3.rs-492231/v1

Abstract

Background: TMZ resistance plays a critical role in the treatment of glioma, our research try to explore how circRNAs affect the chemosensitivity of glioma cells.

Methods: In this study, we proceeded gene sequencing, and selected circRNAs specifically expressed in TMZ resistant cells and use them as target genes for subsequent studies; by knocking out the target gene we clarify its effect on TMZ resistant glioma proliferation, invasion, migration and cell apoptosis; through tumor-burdened animals we explore the effect of target gene in vivo environment.

Results: In our research we revealed that circ-GLIS3 was significantly upregulated in TMZ resistant glioma cells. Functionally, knocking down circ-GLIS3 could inhibit proliferation, invasion, and migration abilities of TMZ resistant glioma cells; moreover, the downregulation of circ-GLIS3 could induce cell cycle arrest and apoptosis, while miR-548m inhibition and MED31 mRNA could reverse this progress. In vivo condition, the silencing of circ-GLIS3 could induce cell apoptosis and suppressed tumor growth. Mechanistically, circ-GLIS3 positively upregulated MED31 expression by sponging miR-548m.

Conclusions: All these research findings demonstrate that circ-GLIS3 accelerates TMZ resistant glioma progression through miR-548m/MED31 axis.

Introduction

Glioma is a tumor which shares malignancy with strong aggressiveness. The mortality rate of glioma has decreased with the improvement of surgery-related technologies and chemoradiotherapy. However, since its diagnosis is incurable, the prognosis of glioma remains poor, patients share only 5.5% in 5 years survival rate (1–3). Temozolomide (TMZ) is recognized as the most common and effective treatment for glioma patients at present (4–7), however about 50% patients treated with TMZ developed chemotherapy resistance, partly owing to the elevated expression of O6-methylguanine methyltransferase (MGMT) and the lack of a DNA repair pathway in tumor cells, prognosis for these patients remains poor (8). All these clinical difficulties remind us we should explore the mechanism of TMZ resistance in glioma.

Exosomes are small, extracellular vesicles with lipid bilayer membranes. When these vesicles incorporate into target cells, vesicular-contented RNA molecules, proteins and lipids will be released into cellular microenvironment, thus mediating cell-cell communication (9–12). Circular RNAs (circRNAs) are novel discovered noncoding RNAs which could function as essential regulators in cancer progression. Up to now, several evidence suggested that tumor-derived exosomes could be engaged in cancer biological processes, including tumor angiogenesis, metastasis and chemoresistance (13–16).

In our previous work, we discovered that circ_0086248 (chr9:4286037–4298496; gene symbol: GLIS3) was obviously increased in A172/TMZ-R cells compared with SVG cells. Functionally, we detected cell proliferation and invasion affected by circRNA-GLIS3 in vitro. Through bioinformatics analysis, we predicted that circRNA-GLIS3 could interact with miR-548m to regulate MED31 expression and ultimately

affect TMZ resistant glioma cells. In the present study, we aim to explore whether circRNA-GLIS3 is involved in TMZ resistance of glioma and attempt to confirm whether circRNA-GLIS3/miR-548m/MED31 signal pathway could promote the malignant biological properties of TMZ resistant glioma cells and clarify their regulatory mechanism. Thus could indicate a potential therapeutic target.

Materials And Methods

TMZ resistant glioma cell culture

A172 and U251 cell lines were incubated in DMEM medium with increasing TMZ concentration, to established TMZ-resistant glioma cells (A172/TMZ-R and U251/ TMZ-R) by stepwise (8 months) increasing exposure (Initially cultured in DMEM medium containing 5 μM of TMZ, and maintain for 2 weeks at each dose; thereafter, the dose gradually increased and finally reached 400 μM). SVG cells were proceeded with adhesive culture.

Isolation and characterization of cell-derived exosomes

We use Hieff™ Quick exosome isolation kit to extract exosomes from A172/TMZ-R, U251/TMZ-R and SVG cell lines. Thirty microliters of exosomes were placed in an EP tube, and RIPA lysis buffer was added. Then, all these reagents were mixed and frozen.

Cell treatment and transfection

For circRNA-GLIS3 knockdown, the TMZ resistant cells were transfected with 20 nM of siRNA against circRNA-GLIS3 (si-circ-GLIS3, GenePharma, Shanghai, China) as treatment group. For circRNA-GLIS3 up-regulation, 50 ng of circRNA-GLIS3 overexpression plasmids (vector-circRNA-GLIS3, GenePharma) were transfected into cells. MiR-548m overexpression or knockdown was achieved using 20 nM of miR-548m mimic (GenePharma) or miR-548m inhibitor (anti-miR-548m, GenePharma). A172/TMZ-R and U251/TMZ-R cells were transduced for 24 hours. Then, we proceeded with qPCR to confirm circRNA/miRNA inhibition in stable cells.

Western blotting

Total proteins were extracted with an extraction kit (supplemented with a protease inhibitor cocktail). The primary antibody was diluted in the appropriate ratio of T-TBS (containing 3% BSA) and incubated at 4°C overnight. The secondary antibody was diluted in the appropriate ratio of T-TBS (containing 3% BSA) in a certain proportion. ECL was used to visualize Western blotting substrate immunoreactive bands.

EdU and clone formation assay

In EDU assay cell nuclei were stained with Hoechst for 15 min. After that, all cells were examined. For clone formation assay, transfected cells were seeded in 6-well plates and cultured in medium containing

10% FBS at 37°C with 5% CO2. Approximately 10 days later, the cells were stained with 0.1% crystal violet (Beyotime, Beijing, China).

CCK-8 assay

Cells were plated into 96-well plates (3000 cells/well). 10 μl of Cell-Counting Kit-8 (Dojindo Laboratories, Kumamoto, Japan) reagent was added after cultured for 24, 48, 72, and 96 hours. Two hours later, the OD value was measured at a wavelength of 450 nm.

Transwell assay

Invasion abilities were tested using a matrigel-coated 24-well transwell plate. Cells in serum-free medium were added to the upper chamber. After culturing for 24 hours, the cells were fixed with methanol and stained with 1% crystal violet. After that, the cells were viewed through a Nikon TE 2000 microscope.

Migration assay

Cells were added after culture plate marking, and were washed with sterile PBS 3 times as a scratch was completed. The cells were cultured in an incubator with 5% CO2 at 37°C. Then, all cells were removed and observed under a microscope after 24 hours.

Cell cycle assay

Examine cells were harvested 48 hours after transfection and washed with PBS, then fixed in 70% ethanol for 24 hours and incubated for 15 mins. Cell cycle was immediately analyzed using a flow cytometer (Millipore Guava).

Apoptosis assay

All samples were analyzed by flow cytometry, the cells were grouped into viable, necrotic, and apoptotic cells, and the percentages of apoptotic cells of each group were counted.

Xenograft model

Ten BALB/c nude mice (200 μL per mouse) aged 3 weeks were randomly divided into two groups. In experimental group, A172/TMZ-R cells were suspended in serum-free DMEM (1×106 to 1×107/mL), after circRNA-GLIS3 was knocked down (inhibitor transfected by lentivirus), we implanted the cells subcutaneously into the right anterior side of nude mice continuously for 5 days. In NC group, the mice were subcutaneously injected with A172/TMZ-R cells (PBS transfected with lentivirus). We chose 6, 12, 18, 24 and 30 days after subcutaneous injection as measurement points, tumor size was measured by caliper, and tumor volume (mm^3) was calculated as follows: length×width2/2. 30 days after injection, the BALB/c nude mice were killed and dissected to remove the subcutaneously implanted tumors, and the tumors were weighed by electronic balance. Pathological sections were made and observed under a microscope after hematoxylin and eosin staining.

Statistical analysis

Data analysis was performed using SPSS18.0. GraphPad 5.0 was applied to present the data analyses. Differences were analyzed by Student's t-test, with P□0.05 indicating statistical significance.

Results

Circ-GLIS3 expression was upregulated in A172/TMZ-R cells and cell-derived exsomes

A172/TMZ-R and SVG cells were identified through microscopic examination (Fig. 1A, B). To determine whether cell-derived exosomes were successfully purified, the exosome morphology was verified under transmission electron microscopy (Fig. 1C, D). CircRNA sequencing was performed in A172/TMZ-R and SVG cell lines. Differential expression was revealed through boxplots, scatter plots, volcano plots and hierarchical clustering (Fig. 1E). Then, primer screening and RT-PCR were conducted to localize candidate circRNAs. According to the relative circRNA expression, we found that circ-GLIS3 was significantly upregulated in A172/TMZ-R cells (both in cells and exsomes).

CircRNA-GLIS3 knockdown inhibited the progression of TMZ resistant glioma cells

To examine the biological function of circ-GLIS3 in TMZ resistant glioma, it was silenced in A172/TMZ-R and overexpressed in U251/TMZ-R cells (Fig. 2A and B). CCK-8 and clone formation assays illustrated that silencing of circ-GLIS3 could suppress A172/TMZ-R cell proliferation, whereas its overexpression could promote U251/TMZ-R cell proliferation (Fig. 2A, B, C, D). Transwell assays revealed that silencing of circ-GLIS3 inhibited A172/TMZ-R cell invasion abilities, while its overexpression promoted the invasion abilities in U251/TMZ-R cells (Fig. 2E, F). These results suggested that circ-GLIS3 may act as a promoter in TMZ-resistant glioma cell progression.

Circ-GLIS3 upregulated MED31 expression by sponging miR-548m in TMZ resistant glioma cells

We assumed that circ-GLIS3 could act as a miRNA sponge to regulate glioma phenotype. Through bioinformatics tool screening, we found that among all candidate miRNAs, miR-548m may act as the downstream target of circ-GLIS3 (https://circinteractome. nia.nih.gov/). The junction sites are UACCUUUG and AUGGAAAC. The downstream target of miR-548m was predicted by TargetScan database, MED31 (Chromosome 17: 6,643, 311-6,651,634) was selected as the downstream target, and the potential junction sites of miR-548m were UACCUUU and AUGGAAA. RT-PCR revealed that miR-548m was markedly decreased while MED31 mRNA was markedly increased in A172/TMZ-R and U251/TMZ-R cells, accompanied with circ-GLIS3 reduction (Fig. 3A, B).

Moreover, in our study, we transfected sh-circ-GLIS3 into A172/TMZ-R cells. The results indicated that circ-GLIS3 knockdown obviously repressed MED31 mRNA expression in TMZ resistant cells, whereas inh-miR548m and MED31 mRNA could rescue this effect. Meanwhile we transfected circ-GLIS3 mimics into U251/TMZ-R cells. The results indicated that circ-GLIS3 overexpression obviously promoted MED31

mRNA expression in TMZ resistant glioma cells, whereas miR548m mimics and MED31 inhibitor could achieve the opposite effect. Overall, these data prove that circ-GLIS3 is targeted by miR-548m as a miRNA sponge to regulate MED31 expression.

At the same time we explored the subcellular location of circ-GLIS3 to investigate its role in glioma progression. The results revealed that circ-GLIS3 was located mostly in the cytoplasm of A172/TMZ-R cells (Fig. 3C), which indicated that circ-GLIS3 could regulate glioma pathological processes in posttranscriptional procedures.

Circ-GLIS3 promoted TMZ resistant glioma cell progression through miR-548m/MED31 axis

In EdU cell proliferation assay, proliferating cell ratio statistically decreased in si-circ-GLIS3 group, in clone formation assay, the results illustrated that silencing of circ-GLIS3 obviously reduced colony-formation ability in A172/TMZ-R and U251/TMZ-R cells (Fig. 4A, B, C, D). In Transwell assay, the number of invasive cells was significantly reduced in si-circ-GLIS3 group (Fig. 4E, F). The scratch assay indicated that circ-GLIS3 knockdown could inhibit cell migration ability (Fig. 4G, H), these results indicated that circ-GLIS3 could promote TMZ resistant glioma cell's proliferation, invasion and migration abilities.

To further verify the regulatory relationship among circ-GLIS3, miR-548m and MED31, we tested the proliferation, invasion and migration abilities of A172/TMZ-R and U251/TMZ-R cells after transfection with inh-miR-548m and MED31 mRNA. The results indicated that the downregulation of miR-548m and upregulation of MED31 could rescue the si-circ-GLIS3-inhibited proliferation, invasion and migration abilities (Fig. 4). Through these cell function assays, we concluded that circ-GLIS3 could promote glioma cell proliferation, invasion and migration through miR-548m/ MED31 axis.

Circ-GLIS3 inhibited cell cycle arrest and cell apoptosis in TMZ resistant glioma cells through miR-548m/MED31 axis

We proceeded flow cytometry to investigate the effects of circ-GLIS3/miR-548m/MED31 signaling pathway on TMZ resistant glioma cell cycle and apoptosis. As shown in Fig. 5A and 5B, the apoptosis ratio was higher in si-circ-GLIS3 group, Moreover the cells in si-circ-GLIS3 group were arrested in G0/G1 phase, meanwhile circ-GLIS3 cells co-transfected with miR-548m inhibitor or MED31 mRNA could reverse this effect. These results proved that circ-GLIS3 may inhibit cell cycle arrest and cell apoptosis in TMZ resistant glioma cells by binding to miR-548m and upregulating MED31 expression.

Downregulation of circ-GLIS3 suppressed TMZ resistant tumor growth in vivo

Nude mouse xenograft tumors were generated to verify the effect of circ-GLIS3 on TMZ resistant glioma proliferation in vivo. In tumor-bearing mice injected with circ-GLIS3-deficient A172/TMZ-R cells, the volume and weight of tumors were markedly smaller than those injected with normal A172/TMZ-R cells (Fig. 6A, C, D). The timing measurements represented a large slowdown in tumor growth (Fig. 6B). HE staining showed that apoptotic cells in subcutaneous tumor sections were obviously increased in the si-

circ-GLIS3 group (Fig. 6E). All these results proved that circ-GLIS3 could promote TMZ resistant glioma cell growth in vivo.

Discussion

High-grade glioma treatment is associated with poor median survival time so a better understanding of its mechanisms is needed to improve the treatment efficacy (17). In clinical work we found that TMZ resistance plays a critical role in the treatment of glioma, but the underlying mechanisms are not fully clarified yet (18–20). Previous studies revealed that the development of high grade glioma is associated with abnormal expression of circRNAs (21–22). Therefore, in this research we try to explore how circRNAs affect the chemosensitivity of glioma cells.

Increasing evidence suggests that exsomes and circRNAs they carried may play important roles in glioma progression. Until now the exact correlation between exsomes, circRNAs and glioma progression is still unclear. Previous studies suggested that exosomes derived from glioma cells could modify recipient cells by transferring proteins, miRNAs and noncoding RNAs (23, 24, 25, 26). Due to their ability to mediate their function by directly binding to miRNAs, circRNAs are considered miRNA sponges and competing endogenous RNAs (ceRNAs) for miRNAs. In osteosarcoma downregulation of circPVT1 enhanced the sensitivity to doxorubicin and cisplatin through downregulating the expression of ATP-binding cassette sub-family B member 1 (27). CircPAN3 functioned as a sponge for miR-153-3p/miR-183-5p to promote ADM resistance in THP-1/ADM cells (28). Furthermore, circRNA-MTO1 is up-regulated in monastrol-resistant breast cancer cells and promoted monastrol resistance through regulating tumor necrosis factor receptor-associated factor 4/kinesin-5 axis (29).

In our previous research, we extracted exosomes from A172/TMZ-R, U251/TMZ-R and SVG cell lines. Through exsome-contained circRNA-seq analysis, we discovered that compared with SVG cells circ-GLIS3 was obviously upregulated in A172/TMZ-R cell lines. According to bioinformatic analysis, circ-GLIS3 harbors a binding site for miR-548m, thus regulate MED31 expression. Previous study revealed that miR-548m expression was downregulated in breast cancer patients, overexpression of miR-548m increased E-cadherin expression and decreased EMT-associated transcription factors expression. Thus could inhibited migration and invasion capabilities of breast cells (30). Jiang reported that downregulation of Med31 suppressed osteosarcoma cell proliferation, and overexpression of Med31 abrogated the effects of miR-1 on cell proliferation (31). Furthermore, the interaction between circ-GLIS3, miR-548m and MED31 was confirmed by luciferase reporter assay, miR-548m was downregulated while MED31 mRNA was upregulated in A172/TMZ-R and U251/TMZ-R cell lines, implicated that circ-GLIS3 may function as a sponge for miR-548m to regulate MED31 expression in TMZ resistant glioma cells. Through primary functional verification, we revealed that circ-GLIS3 silencing could inhibit TMZ resistant glioma proliferation and invasion in vitro.

In this study, Western blotting analysis revealed that the circ-GLIS3 silencing could downregulate MED31 expression, while miR-548m co-silencing and MED31 mRNA partially rescued this reduction. According to

these research findings, we determined that circ-GLIS3 could regulate the MED31 downstream signaling pathway by sponging miR-548m.

By functional verification, we revealed that circ-GLIS3 knockdown could inhibit TMZ resistant glioma proliferation, invasion and migration in vitro, and circ-GLIS3 ornithine decarboxylase could achieve the opposite result. Subsequent interventions showed that reduced miR-548m expression and upregulation of MED31 could rescue si-circ-GLIS3-induced proliferation, invasion and migration ability reduction in TMZ resistant glioma cells. In addition, the reduced expression of circ-GLIS3 could promote glioma cell cycle arrest and cell apoptosis and circ-GLIS3 ODC could lead to the opposite result, meanwhile miR-548m inhibitor or MED31 mRNA could reverse this progression. According to these results, we concluded that circ-GLIS3 could promote proliferation, invasion and migration ability in TMZ resistant glioma cells, and it could also weaken TMZ-induced apoptosis by activating miR-548m/MED31 axis, thus resulting in resistance to TMZ application.

In animal models, we revealed that downregulation of circ-GLIS3 could result in a reduction in tumor volume and weight. HE staining of subcutaneous tumor sections showed that cell apoptosis obviously increased with circ-GLIS3 silencing. This indicated that circ-GLIS3 could promote TMZ resistant tumor growth in vivo.

In summary, our findings revealed the alteration of expression patterns of circRNAs, miRNA and mRNAs in temozolomide-resistant glioma cells, and explored their effect on glioma progression in vitro and vivo condition. After a series of research analysis we demonstrated the following conclusions: First, TMZ resistant glioma cell derived exsome-contained circ-GLIS3 could regulate MED31 expression by sponging miR-548m; second, circ-GLIS3 could promote TMZ resistant glioma proliferation, invasion and migration, it could also inhibited their cell cycle arrest and apoptosis, miR-548m inhibitor or MED31 mRNA could rescue these processes; third, circ-GLIS3 could inhibited TMZ resistant glioma cell apoptosis and promote tumor growth in vivo condition. These findings suggested that circ-GLIS3 could regulate TMZ resistant glioma malignancy through miR-548m/MED31 axis, our research data highlighted a novel mechanism of resistance to TMZ in glioma, which could serve as a potential therapeutic target in the treatment of glioma patients.

Ethics approval and consent to participate

I promise that the study was performed according to international, national and institutional rules considering animal experiments, clinical studies and biodiversity rights. The procedures for the care and use of animals were approved by the Ethics Committee of The Affiliated Suzhou Hospital of Nanjing Medical University, and all applicable institutional and governmental regulations concerning the ethical use of animals were followed (No: JN.No20190325b0460, Date: March 05 2020). All experimental procedures were conducted in accordance with local guidelines on the ethical use of animals and the National Institutes of Health Guide for the Care and Use of Laboratory Animals.

Consent for publication

Not applicable

Declarations

Ethics approval and consent to participate

I promise that the study was performed according to international, national and institutional rules considering animal experiments, clinical studies and biodiversity rights. The procedures for the care and use of animals were approved by the Ethics Committee of The Affiliated Suzhou Hospital of Nanjing Medical University, and all applicable institutional and governmental regulations concerning the ethical use of animals were followed (No: JN.No20190325b0460, Date: March 05 2020). All experimental procedures were conducted in accordance with local guidelines on the ethical use of animals and the National Institutes of Health Guide for the Care and Use of Laboratory Animals.

Consent for publication

Not applicable

Availability of data and materials

The datasets during and/or analyzed during the current study are available from the corresponding author on reasonable request.

Competing interests

Non-financial competing interests.

Funding

This research was supported by the General Project of Natural Science Research in Colleges and Universities of Jiangsu Province (Project No: 19KJD320002).

Authors' contributions

Li Guowei proceeded vitro/vivo experiment and analyzed the results, and performed gene sequencing and analysis. Jin Yanping performed data statistic analysis, review and correct the manuscript. All authors read and approved the final manuscript.

Acknowledgements

I am greatly indebted to those who have instructed and helped me a lot in the past years. And my thanks would go to my beloved family for their loving considerations and great confidence in me all through these years. I also owe my sincere gratitude to my friends and my fellow classmates who gave me their help and time in listening to me and helping me work out my problems during the difficult course of the thesis.

References

1. Weller M, Wick W, Aldape K, Brada M, Berger M, Pfister SM, Nishikawa R, Rosenthal M, Wen PY, Stupp R, Reifenberger G. Glioma. Nat Rev Dis Primers. 2015;1:15017.
2. Lin C, Lin L, Mao S, Yang L, Yi L, Lin X, Wang J, Lin ZX, Lin JM. Reconstituting glioma perivascular niches on a chip for insights into chemoresistance of glioma. Anal Chem. 2018;90:10326–33.
3. Ostrom QT, Gittleman H, Xu J, Kromer C, Wolinsky Y, Kruchko C, Barnholtz-Sloan. JS 2016 CBTRUS statistical report: primary brain and other central nervous system tumors diagnosed in the United States in 2009–2013. Neuro. Oncol. 18 v1–v75.
4. Brada M, et al. 2003 Phase II study of primary temozolomide chemotherapy in patients with WHO grade II gliomas. Ann. Oncol. 14 1715–1721.
5. van Thuijl HF, et al. 2015 Evolution of DNA repair defects during malignant progression of low-grade gliomas after temozolomide treatment. Acta Neuropathol. 129 597–607.
6. Margison GP, Santibanez Koref MF, Povey. AC 2002 Mechanisms of carcinogenicity/chemotherapy by O6-methylguanine. Mutagenesis 17 483–487.
7. Hombach-Klonisch S, et al. 2018 Glioblastoma and chemoresistance to alkylating agents: Involvement of apoptosis, autophagy, and unfolded protein response. Pharmacol. Ther. 184 13–41.
8. Couzin J. Cell biology: the ins and outs of exosomes. Science. 2005;308:1862–3.
9. Raposo G, Stoorvogel W. Extracellular vesicles: exosomes, microvesicles, and friends. J Cell Biol. 2013;200:373–83.
10. Caby MP, Lankar D, Vincendeau-Scherrer C, Raposo G, Bonnerot C. Exosomallike vesicles are present in human blood plasma. Int Immunol. 2005;17:879–87.
11. Simons M, Raposo G. Exosomes–vesicular carriers for intercellular communication. Curr Opin Cell Biol. 2009;21:575–81.
12. Cocucci E, Racchetti G, Meldolesi J. Shedding microvesicles: artefacts no more. Trends Cell Biol. 2009;19:43–51.
13. Hentze MW, Preiss T. Circular RNAs: splicing's enigma variations. EMBO J. 2013;32:923–25.
14. Ashwal-Fluss R, Meyer M, Pamudurti NR, Ivanov A, Bartok O, Hanan M, Evantal N, Memczak S, Rajewsky N, Kadener S. circRNA biogenesis competes with pre-mRNA splicing. Mol Cell. 2014;56:55–66.
15. Thomson DW, Dinger ME. Endogenous microRNA sponges: evidence and controversy. Nat Rev Genet. 2016;17:272–83.
16. Ebbesen KK, Kjems J, Hansen TB. Circular RNAs: identification, biogenesis and function. Biochim Biophys Acta. 2016;1859:163–68.
17. Li B, Huang MZ, Wang XQ, Tao BB, Zhong J, Wang XH, Zhang WC, Li ST. TMEM140 is associated with the prognosis of glioma by promoting cell viability and invasion. J Hematol Oncol. 2015;8:89.

18. Zhang L, Yang H, Zhang W, Liang Z, Huang Q, Xu G, Zhen X, Zheng LT. Clk1-regulated aerobic glycolysis is involved in glioma chemoresistance. J Neurochem. 2017;142:574–88.
19. Yu Z, Xie G, Zhou G, Cheng Y, Zhang G, Yao G, Chen Y, Li Y, Zhao G. NVP-BEZ235, a novel dual PI3K-mTOR inhibitor displays anti-glioma activity and reduces chemoresistance to temozolomide in human glioma cells. Cancer Lett. 2015;367:58–68.
20. Xu C, Yu Yand Ding F. Microarray analysis of circular RNA expression profiles associated with gemcitabine resistance in pancreatic cancer cells. Oncol Rep. 2018;40:395–404.
21. Li J, Zhu Y, Wang H, Ji X. Targeting Long Noncoding RNA in Glioma: A Pathway Perspective. Mol Ther Nucleic Acids. 2018;13:431–41.
22. Mercer TR, Dinger ME, Mattick JS. Long non-coding RNAs: insights into functions. Nat Rev Genet. 2009;10(3):155–9.
23. Domenis R, Cesselli D, Toffoletto B, et al. Systemic T Cells Immunosuppression of Glioma Stem Cell-Derived Exosomes Is Mediated by Monocytic Myeloid-Derived Suppressor Cells. PLoS One. 2017;12(1):e0169932.
24. Gong M, Yu B, Wang J, Wang Y, Liu M, Paul C, Millard RW, Xiao DS, Ashraf M, Xu M. Mesenchymal stem cells release exosomes that transfer miRNAs to endothelial cells and promote angiogenesis. Oncotarget. 2017;8(28):45200–12.
25. Li MY, Liu DW, Mao YG. Advances in the research of effects of exosomes derived from stem cells on wound repair. Zhonghua Shao Shang Za Zhi. 2017;33(3):180–4.
26. Figueroa J, Phillips LM, Shahar T, Hossain A, Gumin J, Kim H, Bean AJ, Calin GA, Fueyo J, Walters ET, et al. Exosomes from glioma-associated mesenchymal stem cells increase the Tumorigenicity of glioma stem-like cells via transfer of miR-1587. Cancer Res. 2017;77(21):5808–19.
27. Kun-Peng Z, Xiao-Long M, Chun-Lin Z. 2018 Overexpressed circPVT1, a potential new circular RNA biomarker, contributes to doxorubicin and cisplatin resistance of osteosarcoma cells by regulating ABCB1. Int. J. Biol. Sci. 14 321–330.
28. Shang J, Chen WM, Wang ZH, Wei TN, Chen ZZ, Wu WB. CircPAN3 mediates drug resistance in acute myeloid leukemia through the miR-153-5p/miR-183-5p-XIAP axis. Exp Hematol. 2019;70:42–54.
29. Liu Y, Dong Y, Zhao L, Su L, Luo J. Circular RNAMTO1 suppresses breast cancer cell viability and reverses monastrol resistance through regulating the TRAF4/Eg5 axis. Int J Oncol. 2018;53:1752–62.
30. Wm Nor WMFSB, Chung I, Said NABM. MicroRNA-548m Suppresses Cell Migration and Invasion by Targeting Aryl Hydrocarbon Receptor in Breast Cancer Cells. Oncol Res. 2021 Mar 16;28(6):615–629.
31. Jiang C, Chen H, Shao L, Wang Q. MicroRNA-1 functions as a potential tumor suppressor in osteosarcoma by targeting Med1 and Med31. Oncol Rep. 2014 Sep;32(3):1249–56.

Figures

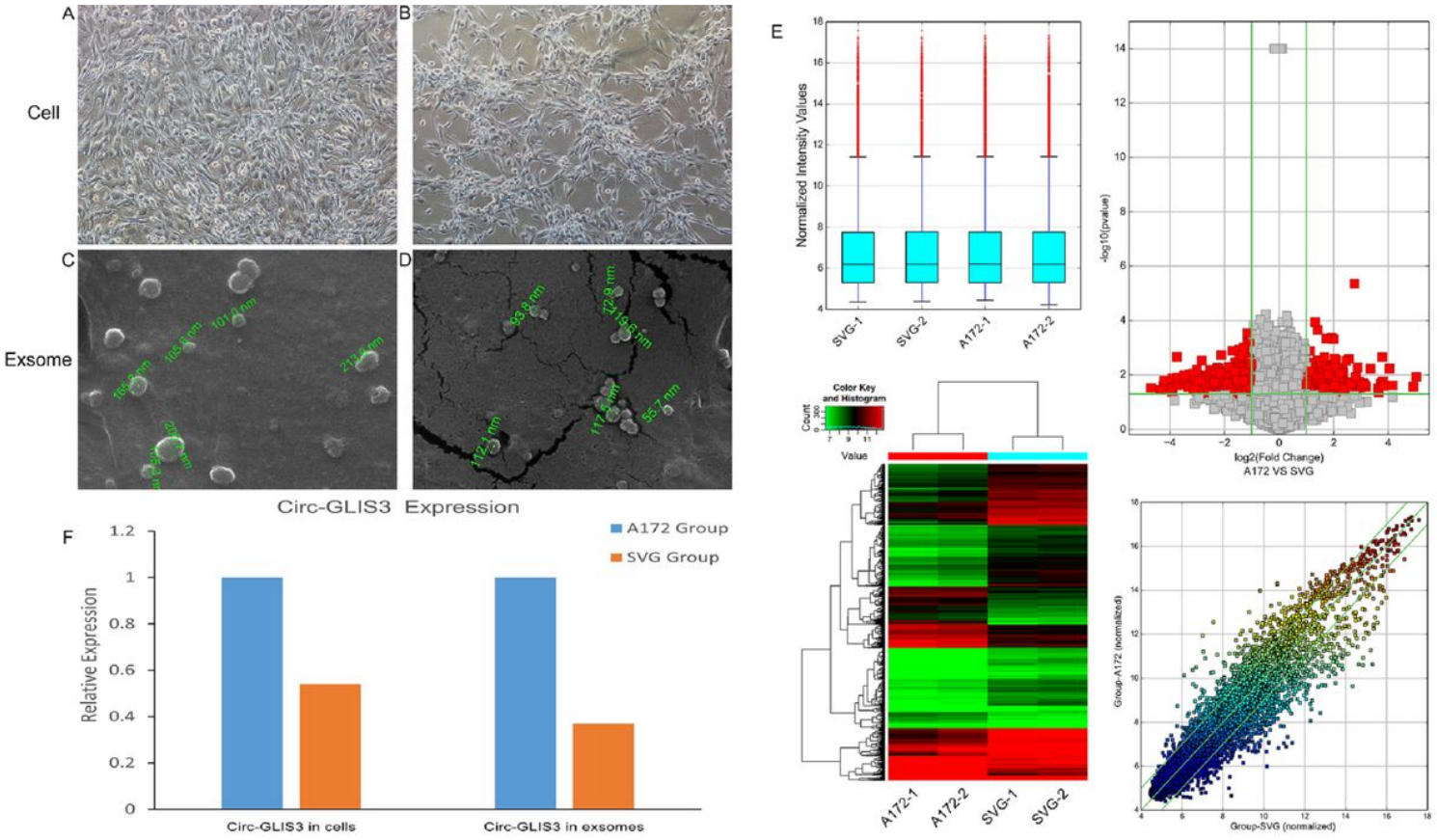

Figure 1

Circ-GLIS3 expression is up-upregulated in A172/TMZ-R cells A. A172/TMZ-R cells before sample collection. B. SVG cells before sample collection. C+D. TEM observation of A172/TMZ-R and SVG derived exosomes. E. Boxplot of A172/TMZ-R and SVG cirRNA-seq; volcano plot of cirRNA-seq, upregulated (right side red), downregulated (left side red) or unchanged (gray); hierarchical cluster analysis presented significantly upregulated/downregulated circRNAs between A172/TMZ-R and SVG cells; scatter plot of A172/TMZ-R and SVG cirRNA-seq. F. Circ-GLIS3 expression was detected after transfection by qRT-PCR.

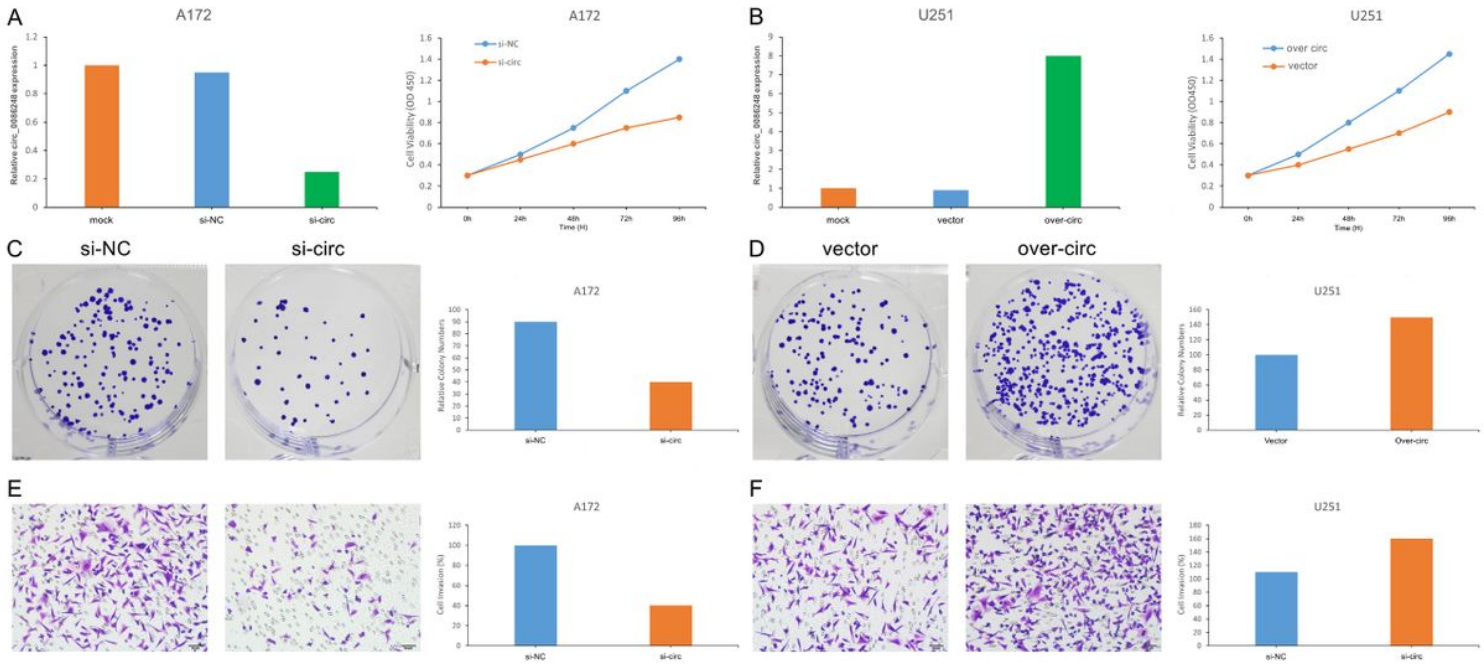

Figure 2

Circ-GLIS3 promotes glioma cell progression A+B. Circ-GLIS3 expression was detected after transfection in A172/TMZ-R and U251/TMZ-R cells by qRT-PCR; CCK-8 assays were used to detect cell viability after transfection. C+D. Colony formation assays were used to detect the clone ability after transfection. E+F. Transwell assays were used to detect cell invasion capacities after transfection. The results indicated that circ-GLIS3 could promote glioma cell progression in vitro, magnification, ×10.

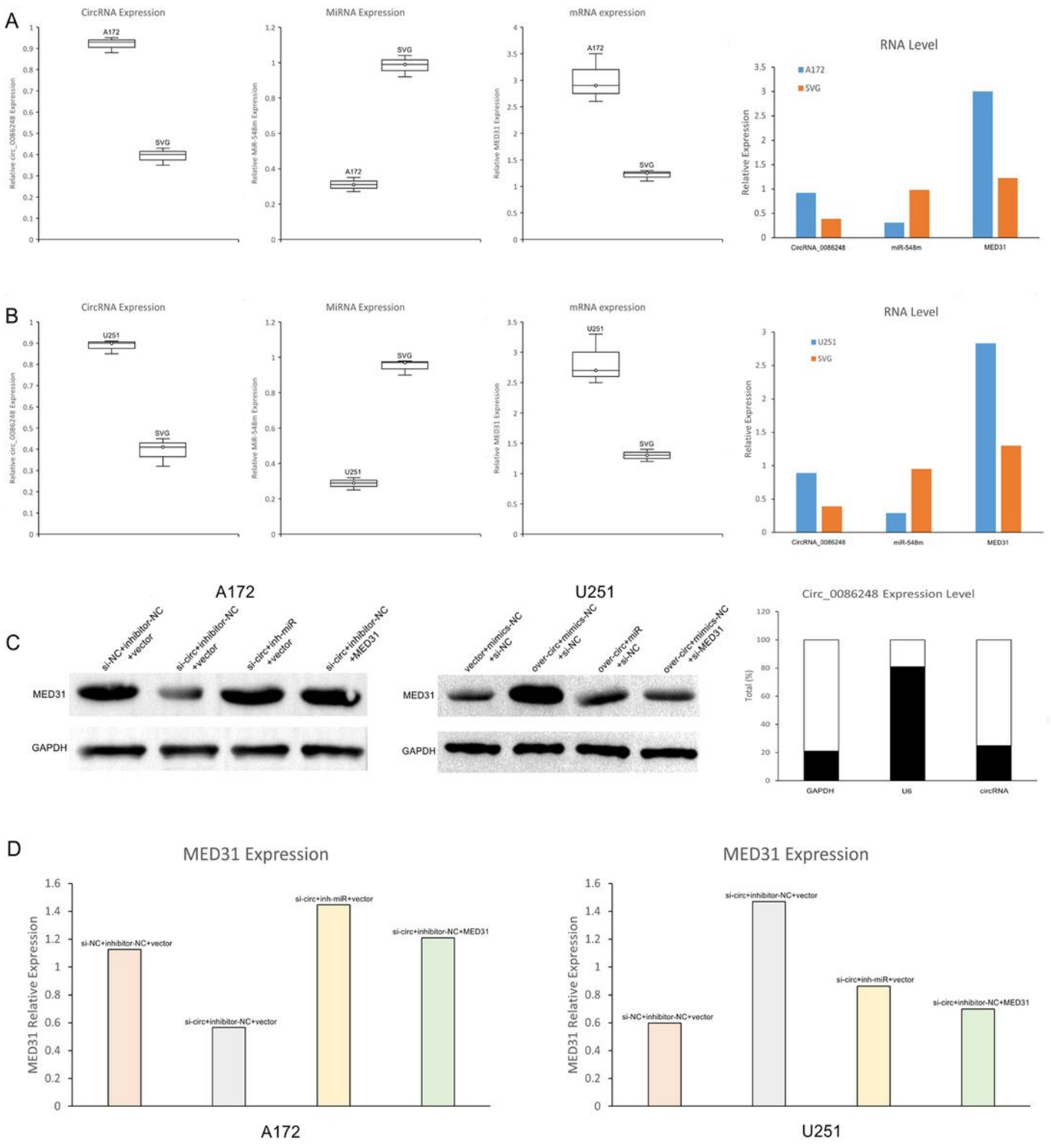

Figure 3

Circ-GLIS3 upregulated MED31 expression by sponging miR-548m A+B. Relative circ-GLIS3, miR-548m and MED31 mRNA expression was detected by qRT-PCR in A172/TMZ-R and U251/TMZ-R cells. C+D. MED31 expression was detected by Western Blot assays after transfection. Results indicated that silencing of circ-GLIS3 could downregulate MED31 expression, while co-transfected with miR-591 inhibitor and MED31 mRNA could reverse this effect; meanwhile circ-GLIS3 over-expression could

upregulate MED31 expression, while co-transfected with miR-591 mimics and MED31 inhibitor could reverse this effect; the circRNA expression levels were assessed by qRT-PCR, GAPDH was used as cytoplasmic markers and U6 was used as nuclear markers.

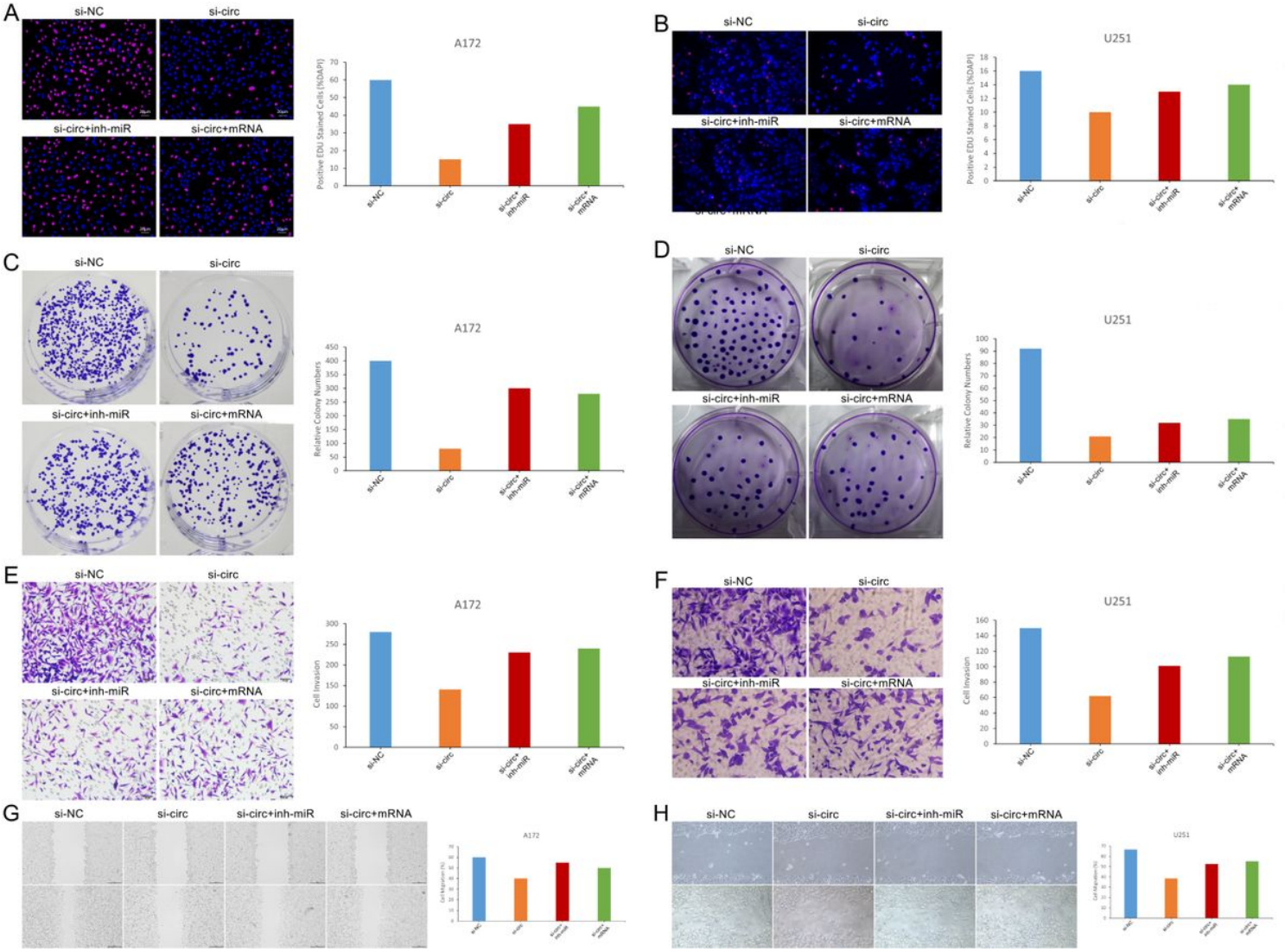

Figure 4

Circ-GLIS3 promoted proliferation, invasion and migration capacities of glioma cells through miR-548m/MED31 axis A+B+C+D. EdU and Colony formation assays showed that knockdown of circ-GLIS3 inhibited cell proliferation, while co-transfecting with miR-548m inhibitor or MED31 mRNA plasmid abolished the decreased proliferation. E+F. Cell invasion assays showed that knockdown of circ-GLIS3 inhibited cell invasion, while co-transfecting with miR-548m inhibitor or MED31 mRNA plasmid promoted cell invasion. G+H. Scratch test was used to detect the migration ability after transfection (0 hour, 24 hours). The result shows that knockdown of circ-GLIS3 inhibited cell migration, while co-transfecting with miR-548m inhibitor or MED31 mRNA plasmid promoted cell migration. Pictures were captured under a light microscope with the magnification, ×10.

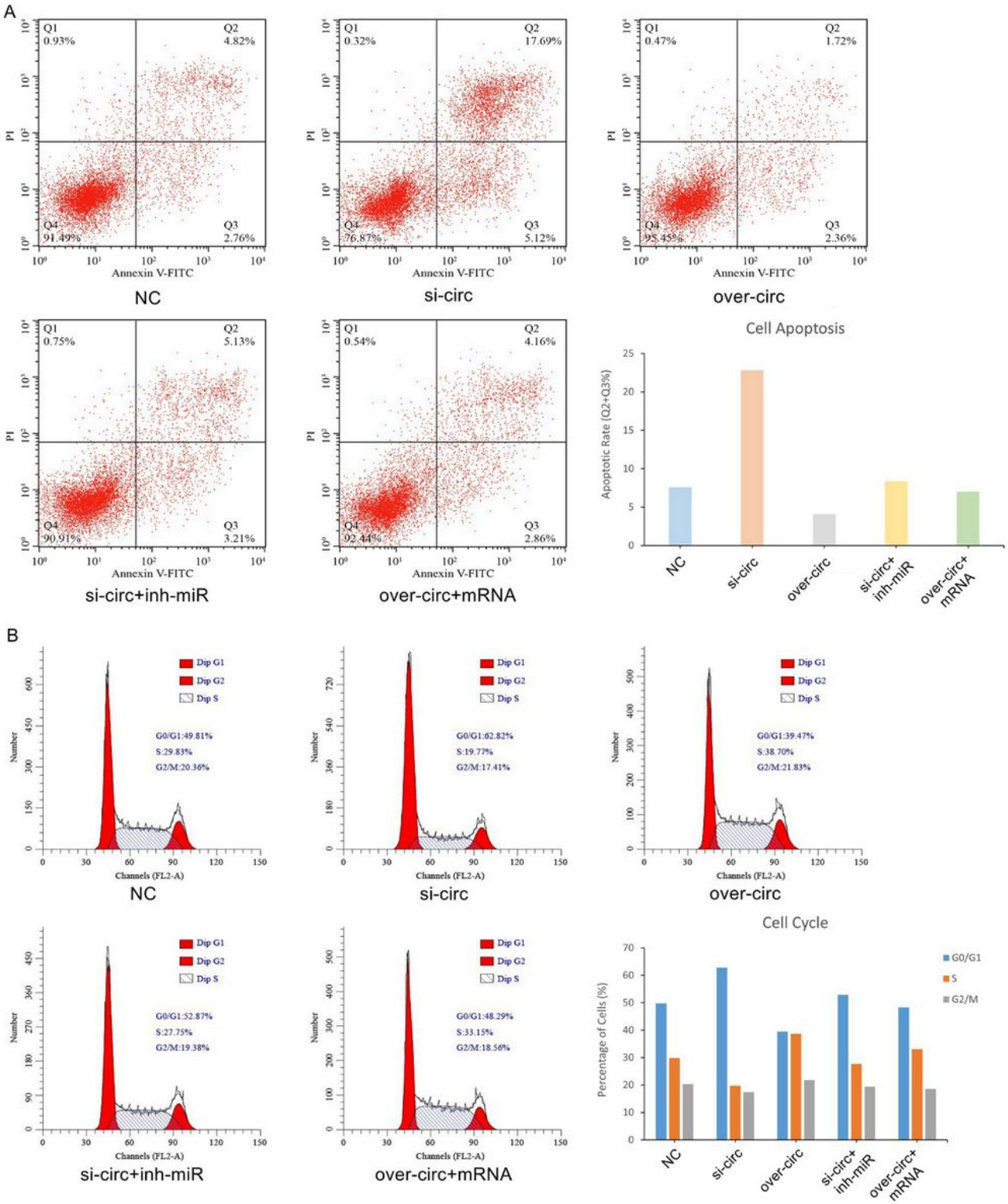

Figure 5

Circ-GLIS3 inhibited cell apoptosis and promoted cell cycle through miR-548m/MED31 axis A. Flow cytometric assay was performed to detect cell apoptosis after transfection. Cell apoptosis assays showed that knockdown of circ-GLIS3 induced cell apoptosis. While co-transfecting with miR-548m inhibitor or MED31 mRNA plasmid reversed this effect. B. Cell cycle assays showed that knockdown of

circ-GLIS3 induced cell cycle arrest. While co-transfecting with miR-548m inhibitor or MED31 mRNA plasmid reversed this effect.

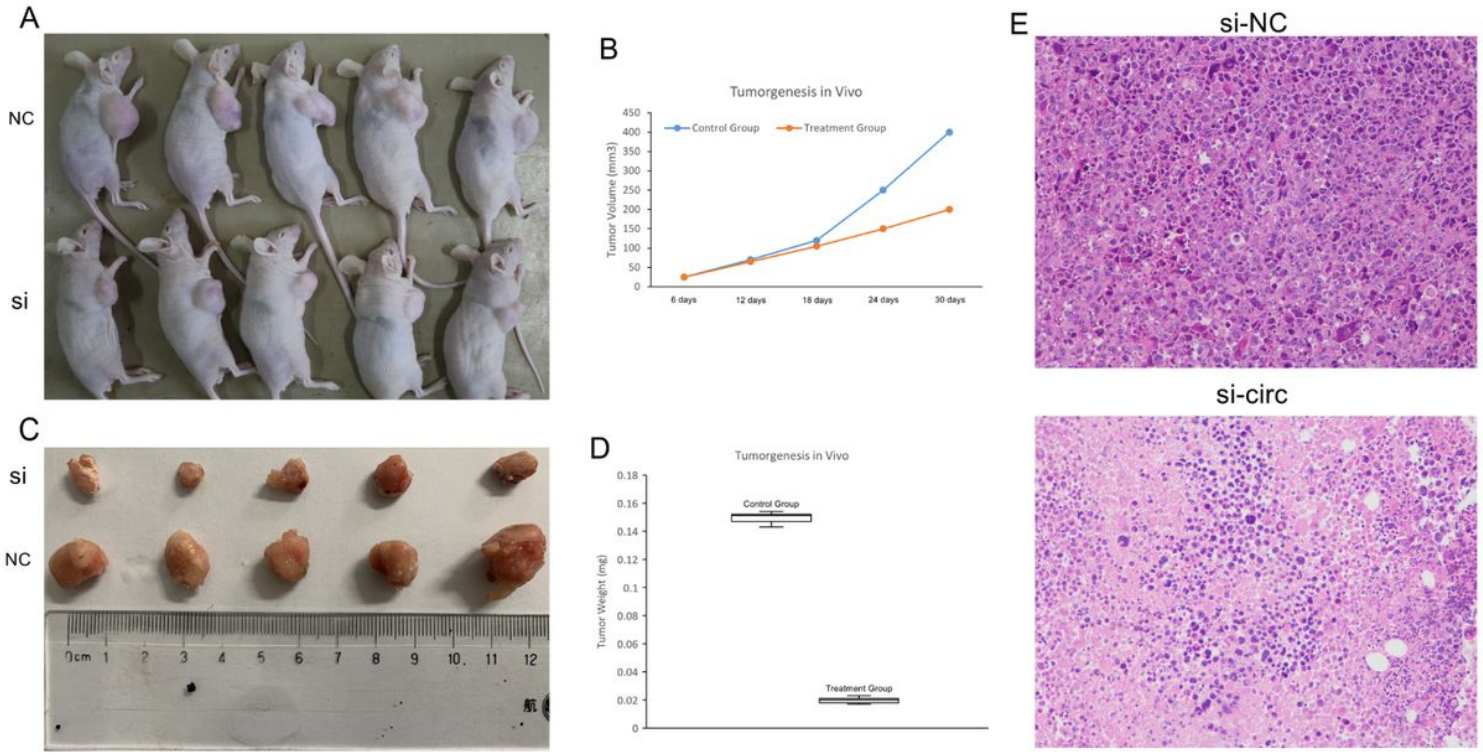

Figure 6

Circ-GLIS3 promoted glioma growth in vivo. A. It shows that the tumor of si-circ-GLIS3 group is smaller than NC group, indicated that downregulation of circ-GLIS3 inhibited glioma proliferation in subcutaneous tumor formation assay; B. Results showed that the growth rate was significantly decreased in si-circ-GLIS3 group; C+D. Tumors were harvested in day 30, results showed that tumor weight was significantly decreased in si-circ-GLIS3 group; E. HE dye for subcutaneous tumor, the result shows that the apoptosis tumor cell increases in si-circ-GLIS3 group.